A Triple Hybrid Framework for Meteorological Drought Modeling in Khuzestan Province, Iran

Sadaf Piri[1], **Mohammad Ansari Ghojghar**[2,*]

1. Ph.D. candidate, Department of Reclamation of Arid and Mountainous Regions Engineering, Faculty of Natural Resources, University of Tehran, Tehran, Iran.

2. Corresponding Author, Assistant Professor, Department of Reclamation of arid and mountainous regions Engineering, Faculty of Natural Resources, University of Tehran, Tehran, Iran.

* Corresponding Author: Ansari.ghojghar@ut.ac.ir

Abstract

Meteorological drought forecasting is essential for sustainable water resources management and climate risk mitigation in arid and semi-arid regions. This study evaluates the performance of hybrid machine learning and time-series approaches for meteorological drought forecasting in Khuzestan Province, Iran. Monthly precipitation data collected from eight synoptic stations during the 1989–2020 period were used to calculate the Standardized Precipitation Index (SPI) at 1-, 3-, 6-, and 12-month time scales. The proposed hybrid framework integrates ARMA-based temporal dependency analysis, GPR nonlinear learning capability, and AF-based adaptive optimization to improve drought forecasting accuracy. Several standalone and hybrid forecasting models were evaluated using the correlation coefficient (R), root mean square error (RMSE), Nash–Sutcliffe efficiency (NS), and mean absolute error (MAE) indices. The results demonstrated that longer temporal scales, particularly SPI-12 and SPI-6, provided more reliable forecasting performance compared with shorter-term indices. Among the investigated models, the proposed triple hybrid framework achieved the highest predictive accuracy across most stations and SPI time scales. For example, under SPI-12 conditions at Bostan station, the proposed framework achieved R, RMSE, NS, and MAE values of 0.922, 0.177, 0.949, and 0.145, respectively, compared with 0.896, 0.215, 0.909, and 0.185 obtained by the ARMA-AF model. The findings highlight the potential of structured hybrid forecasting frameworks for improving meteorological drought prediction reliability in climatically complex regions.

Keywords: Autoregressive Moving Average Model, Gaussian Process Regression, Machine Learning Model, Prediction Models

Introduction

Meteorological drought is one of the most complex and destructive natural hazards, significantly affecting water resources, agricultural productivity, ecosystems, and socio-economic systems worldwide. It is primarily driven by prolonged precipitation deficits and is strongly influenced by climatic variability, particularly in arid and semi-arid regions. In recent decades, the frequency, duration, and severity of drought events have increased due to climate variability and global climate change, making drought forecasting a critical component of water resources management and risk mitigation strategies (Adnan et al. 2023; Sun et al. 2022; Das et al. 2020; Chang et al. 2021). In water-limited environments, drought conditions can severely impact groundwater reserves, river discharge, agricultural production, ecological stability, and human livelihoods (Bond et al. 2008; Hisdal et al. 2001; Wilhite et al. 2007). Therefore, reliable drought prediction models are essential for effective planning and decision-making in drought-prone regions (Negahban et al. 2024; Moisa et al. 2022).

Pre-publication Version

Drought forecasting approaches are generally classified into three main categories: traditional statistical models, machine learning techniques, and hybrid frameworks. Statistical models, such as autoregressive moving average (ARMA), are widely used for modeling linear temporal dependencies in hydroclimatic time series. However, their ability to capture nonlinear and complex drought dynamics is limited. On the other hand, machine learning methods, including Gaussian Process Regression (GPR), support vector regression, and neural networks, provide strong capabilities for modeling nonlinear relationships in climatic data. Nevertheless, these approaches may suffer from overfitting, sensitivity to data quality, and limited interpretability, particularly in small or noisy datasets. To overcome these limitations, hybrid models have been increasingly proposed, combining the strengths of different methods to improve forecasting accuracy and robustness.

In recent years, numerous studies have investigated drought forecasting using different modeling frameworks. For example, ARMA-based models have demonstrated reasonable performance in capturing temporal patterns of the Standardized Precipitation Index (SPI), while hybrid ARMA-GARCH and wavelet-based models have shown improved predictive accuracy compared to standalone statistical approaches (Liu et al. 2019). In addition, machine learning-based methods have been widely applied for drought prediction in different regions, showing strong capability in capturing nonlinear relationships between climatic variables and drought indices (Shamloo et al. 2023; Babaali et al. 2024). Furthermore, several studies have reported that hybrid and ensemble approaches, including wavelet-based and evolutionary optimization techniques, can significantly enhance drought forecasting performance by integrating complementary modeling strengths (Belayneh et al. 2016; Mohammadi et al. 2022; Mousazadeh et al. 2023). Despite these advancements, most existing studies have focused on either single-model approaches or dual hybrid structures, which may not fully capture the complex interaction between linear temporal dependence, nonlinear behavior, and residual error structures in drought processes.

Khuzestan Province, located in southwestern Iran, represents one of the most climatically vulnerable regions in the country. The region is characterized by a transition between arid and semi-arid climates, strong dependence on major river systems such as Karun and Karkheh, and high sensitivity to precipitation variability. These characteristics make the region highly prone to frequent and severe drought events with strong spatial and temporal variability. As a result, conventional or general-purpose drought forecasting models may not be sufficient to accurately represent the complex hydroclimatic behavior of this region, highlighting the need for more advanced and adaptive modeling frameworks tailored to local conditions.

Despite extensive research on drought modeling, there remains a gap in the development of integrated multi-component hybrid frameworks that simultaneously combine temporal dependency modeling, nonlinear learning, and adaptive optimization mechanisms. Most existing approaches do not fully exploit the complementary strengths of these modeling paradigms within a unified framework, particularly in climatically heterogeneous regions such as Khuzestan Province.

Pre-publication Version

To address this gap, the present study proposes a novel triple hybrid framework for meteorological drought forecasting by integrating ARMA, Gaussian Process Regression (GPR), and an adaptive optimization mechanism (AF). The proposed framework aims to improve prediction accuracy by simultaneously capturing linear temporal structures, nonlinear relationships, and optimizing model parameters through adaptive learning. The main contributions of this study are: (1) development of a novel integrated triple hybrid drought forecasting framework; (2) evaluation of model performance across multiple SPI time scales (1-, 3-, 6-, and 12-month); and (3) assessment of the model's applicability in a climatically complex and drought-prone region. The findings of this study are expected to provide useful insights for improving drought monitoring, forecasting, and water resources management strategies in arid and semi-arid environments.

Materials and Methods

Khuzestan Province, covering an area of 64,057 km², is located in southwestern Iran between 31°47′N and 33°04′N latitude and 47°41′E and 50°39′E longitude. The province is bordered by the Zagros Mountain range to the north and east, where elevations gradually decrease toward the southwestern plains. Approximately two-fifths of the province consists of mountainous terrain, primarily concentrated in the northern and eastern regions. Due to its climatic heterogeneity, dependence on major river systems, and high sensitivity to precipitation variability, Khuzestan Province is considered one of the most drought-vulnerable regions in Iran. Fig. 1 illustrates the geographical location of the study area and the spatial distribution of the selected meteorological stations.

Monthly precipitation data used in this study were obtained from eight synoptic stations of the Iran Meteorological Organization (IMO), including Dezful, Bostan, Abadan, Omidieh, Masjed Soleiman, Bandar Mahshahr, Ahvaz, and Ramhormoz. The statistical period of the study spans from 1989 to 2020.

To ensure the reliability and consistency of the precipitation records, a multi-step quality control (QC) procedure was applied. The QC process included standard range and step tests, outlier detection using the interquartile range (IQR) method, and internal consistency evaluation. Missing data handling was performed systematically; short gaps containing fewer than three consecutive observations were reconstructed using linear interpolation, whereas longer gaps were treated as missing values (NA) and excluded from the analysis to minimize potential bias in the forecasting process.

Before model development, the statistical characteristics of the time series were examined. The Run Test was employed to evaluate the homogeneity and randomness of the data at the 95% confidence level. In addition, time-series decomposition was conducted in R software to identify trend, seasonal, and residual components. The stationarity of the SPI series, which is a prerequisite for ARMA modeling, was evaluated using the Augmented Dickey–Fuller (ADF) test.

Pre-publication Version

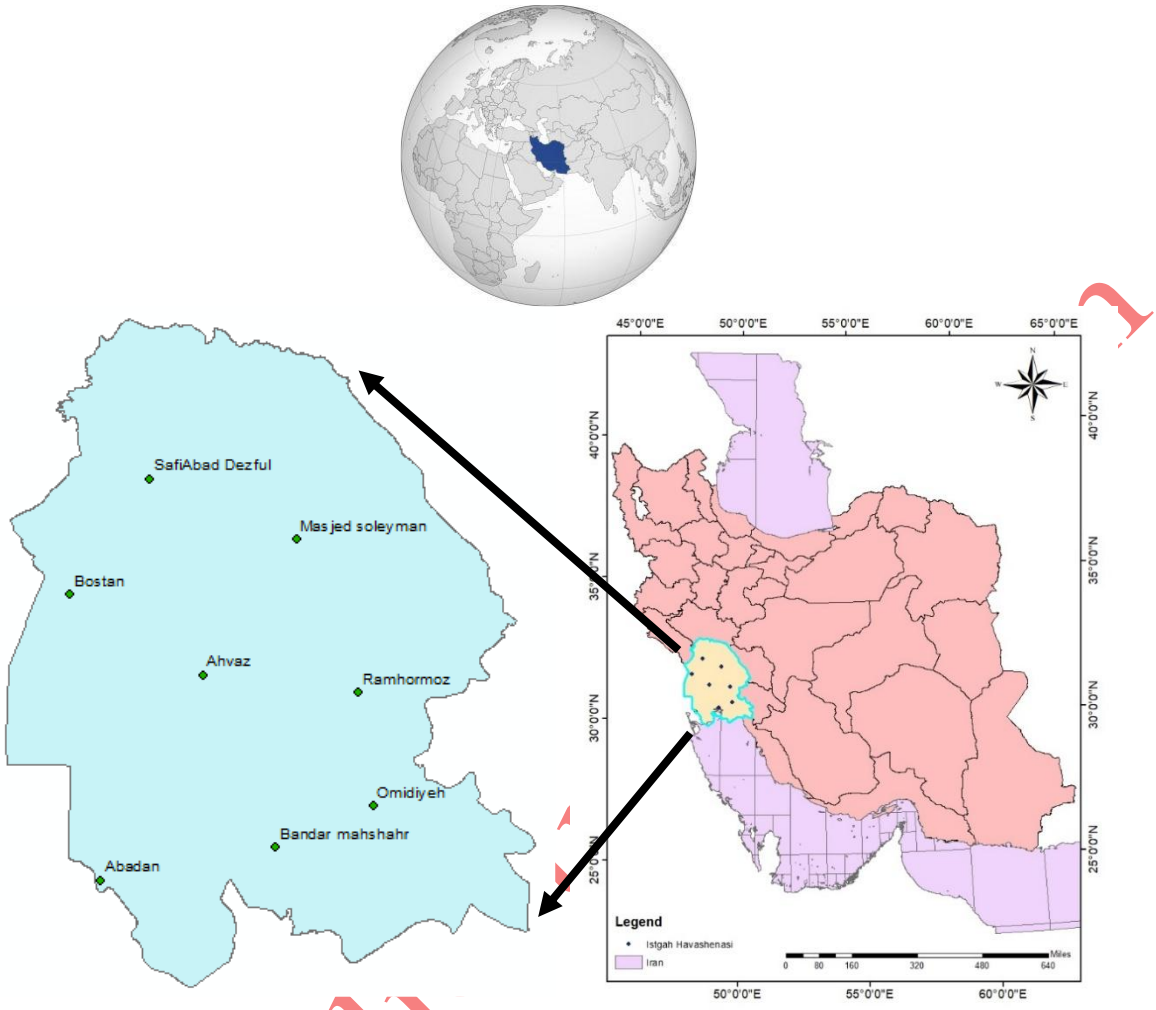


Fig 1. Location map of study area and selected stations

In the present study, precipitation data over 30 years (1989-2020) were used to extract drought ranges from eight meteorological stations located in Khuzestan Province. In the next step, after receiving and preparing precipitation data from the country's meteorological website, the Standardized Precipitation Index values were calculated to distinguish dry and wet years. This index is used to assess drought and can be used to measure the onset time, severity, and duration of drought in different time periods. Given the standardized nature of this index, its most fundamental strength is the ability to compare drought characteristics across time and space, as well as across climate types. To evaluate this index, monthly rainfall values or total rainfall in the considered time periods can be calculated. This index is calculated through relation 1, and its classification is presented in Table 1 (McKee et al. 1993).

$$SPI = \frac{(P - \mu)}{S} \quad (1)$$

P is the amount of precipitation per month, μ is the long-term average precipitation, and S is the standard deviation of the amount of precipitation.

Pre-publi

Table 1. Drought classification based on the SPI value (McKee et al. 1993)

SPI values	2.00 or more	1.50 to 1.99	1.00 to 1.49	0.0 to 0.99	0.0 to -0.99	-1.00 to -1.49	-1.50 to -1.99	-2.00 or less
Drought classification	Extreme Wet	Severe Wet	Moderate Wet	Mild Wet	Mild Drought	Moderate Drought	Severe Drought	Extreme Drought

Gaussian Process Regression (GPR): This method is one of the most desirable and flexible methods in the field of machine learning that operates based on the Bayesian framework. Gaussian process regression is used to model complex and nonlinear relationships between variables without the need to explicitly specify the function structure, and is therefore very suitable for modeling climatic phenomena such as drought. In GPR, instead of assuming a specific function between the input and output, it is assumed that the objective function F(x) follows a Gaussian process, which is described by the following relation:

$$f(x) \sim GP(m(x), k(x, x')) \quad (2)$$

where m(x) is the mean function and k(x, x ′) is the covariance or kernel function. In most cases, the mean function is assumed to be zero, and the modeling information is stored in the kernel function (Zhu et al. 2019).

AF algorithm: The optimization phase of the Triple Hybrid GPR-AF-ARMA Model utilizes an evolutionary computation technique inspired by botanical processes, specifically the Artificial Plant Algorithm (APA), often referred to as the Artificial Flora Algorithm (AFA) or Artificial Plant Optimization Algorithm (APOA) in the literature. This metaheuristic approach is fundamentally inspired by the life cycle and growth characteristics of real plants, such as their propagation strategies, resource acquisition, and spatial distribution. The core mechanism of APA typically involves modeling distinct operational phases: Initialization (Seeding/Original Plants), where a set of initial candidate solutions, termed Original Plants or Seeds, are randomly distributed within the search space corresponding to the model parameters (e.g., GPR kernel parameters or ARMA orders); Growth and Adaptation (Propagation/Growing), where plants iteratively improve their positions in the solution space by mimicking natural processes, often involving mechanisms for propagation (generating Offspring Plants) and calculating propagation distances based on their current fitness (performance metric, such as drought prediction error); and Reproduction/Resource Management (Fruiting), where successful plants (those with high fitness) contribute to the next generation, potentially leading to the replacement of poorer solutions. This stage ensures the exploitation of promising areas found during the search. The APA is employed here as a robust global optimization tool to fine-tune the hyperparameters of the combined GPR and ARMA components within the hybrid framework. By leveraging its mechanisms for exploration (seeding new areas) and exploitation (refining existing high-performing solutions), the APA ensures that the final model configuration achieves superior predictive accuracy for meteorological drought modeling in the Khuzestan Province (Dehghani et al., 2020).

Pre-publication Version

ARMA model: The ARMA model is a stochastic time series model that has been widely used in simulating synthetic weather and meteorological series, especially on monthly and annual scales. The general form of this model is given by the equation (Das et al. 2020):

$$z_t = \varphi_1 z_{t-1} + \cdots + \varphi_p z_{t-p} + \sigma_\varepsilon \xi_t - \theta_1 \varepsilon_{t-1} - \theta_2 \varepsilon_{t-2} - \cdots \theta_q \varepsilon_{t-q} \quad (3)$$

In this model, zt is the standard normal variable at time step t. $\varphi 1$ to φp are the coefficients of the autocorrelated part, and $\theta 1$ to θq are the coefficients of the moving average part of the model. εt is the residual at time step t. $\sigma\varepsilon$ is the standard deviation of the errors, and ξt is the standard normal random variable. p and q are the autoregressive and the moving average of the model, respectively (Liu et al. 2019).

Forecasting Models: In the present study, SPI forecasting models with time windows of 1, 3, 6, and 12 months were used. For example, the first model predicts that the SPI12 level at time t+1 (future) is a function of the SPI12 level at time t (present). In other words, the model uses SPI12 data at time t as input and, using the algorithms in question, predicts the SPI12 level at time t+1. In other models, this is also done based on their time window.

$$SPI_{12(t+1)} = f\left(SPI_{12,t}\right) \quad \text{Model 1}$$
$$SPI_{6(t+1)} = f\left(SPI_{6,t}\right) \quad \text{Model 2}$$
$$SPI_{3(t+1)} = f\left(SPI_{3,t}\right) \quad \text{Model 3}$$
$$SPI_{1(t+1)} = f\left(SPI_{1,t}\right) \quad \text{Model 4}$$

The flow chart of the present study is shown in Fig. 2.

Pre-publication version

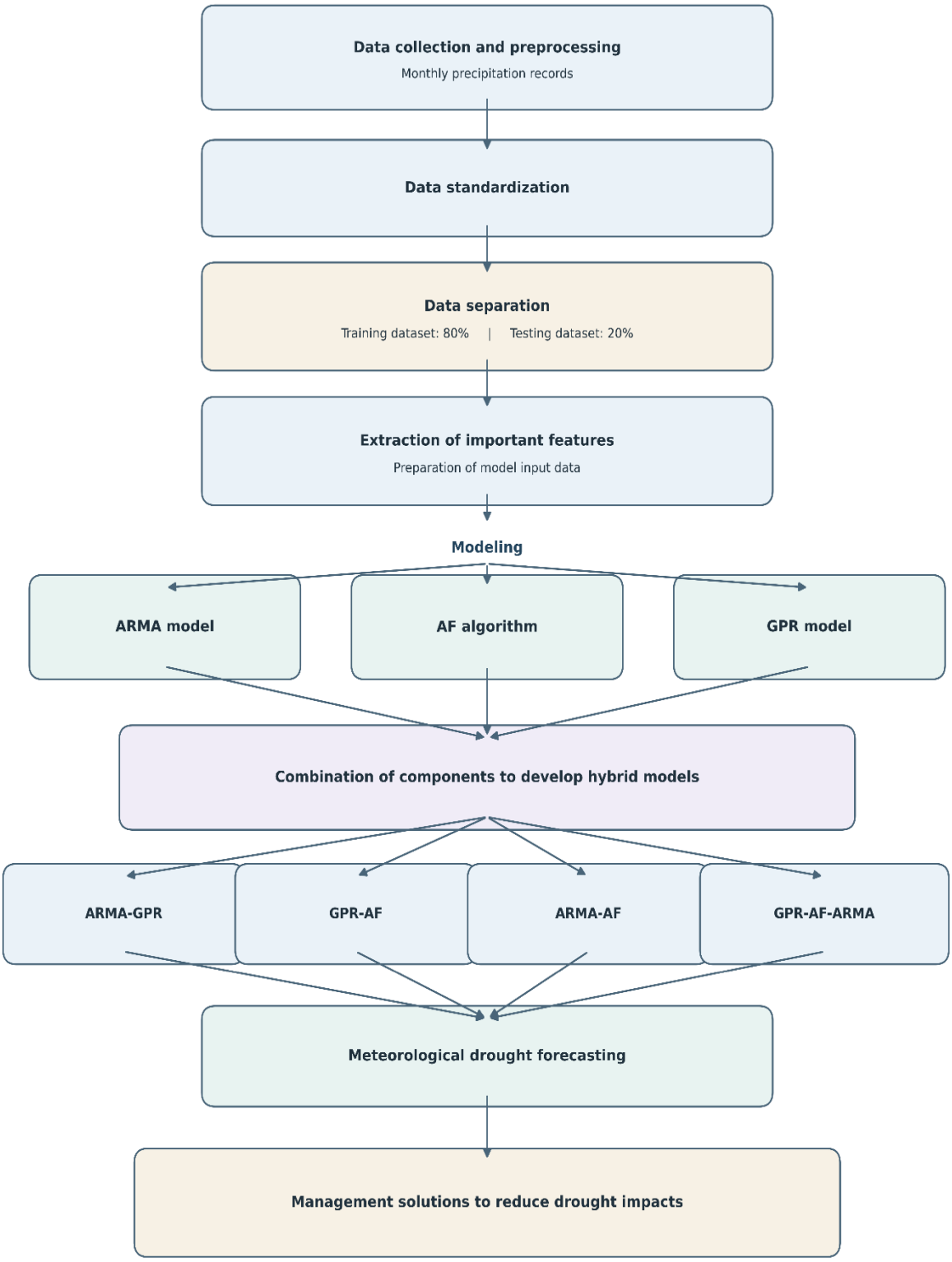


Fig 2. Flowchart of modeling steps with hybrid models ARMA-GPR, GPR-AF, ARMA-AF, and GPR-AF-ARMA

Results and Discussion

Fig. 3 shows the meteorological drought zoning of the stations under study during the specified statistical period.

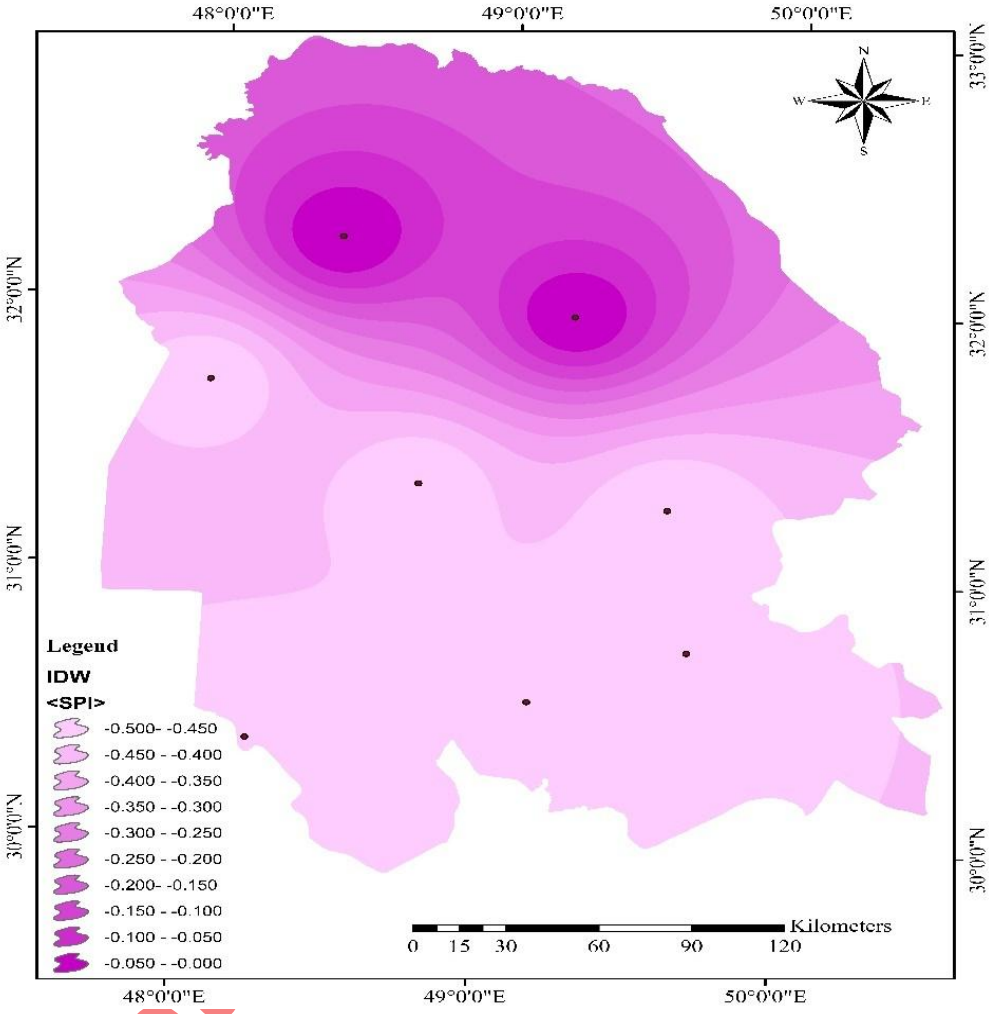


Fig 3. Zoning of meteorological drought at the studied stations during the statistical period

The results obtained from calculating the evaluation criteria R, RMSE, NS, and MAE to determine the best model are presented in Tables 2 to 7. Based on the aforementioned tables and considering the results obtained from the goodness-of-fit evaluation criteria at the eight study stations, in general, the 12-month and 6-month SPIs provided better results and higher accuracy than the 3-month and 1-month SPIs. In comparing the 12-month SPI with the 6-month SPI, the 12-month SPI also showed better performance. For example, the statistical results of the input data to the individual ARMA model at Abadan station showed that using the 12-month SPI instead of the 1-month SPI reduced the RMSE and MAE values from 0.419 and 0.392 to 0.403 and 0.376, respectively. In addition, the R and NS values also increased from 0.528 and 0.588 to 0.543 and 0.612. This can be explained by the fact that meteorological droughts are phenomena with cumulative effects. Shorter time periods (such as 1 or 3 months) may reflect short-term fluctuations

in precipitation that do not necessarily indicate the onset or continuation of a sustained drought period. In contrast, SPI with longer time periods takes into account the cumulative effects of precipitation deficits over a longer time scale and therefore provides a more accurate and consistent picture of the drought situation. The results also showed that combining the AF catalyst with the Box-Jenkins ARMA model strengthened and increased the accuracy of the ARMA model, and this difference was significant at the 95% level. For example, the statistical results of the input data to the ARMA-AF hybrid model at Abadan station showed that using the 12-month SPI instead of the 1-month SPI reduced the RMSE and MAE values from 0.227 and 0.196 to 0.213 and 0.184, respectively. In addition, the R and NS values also increased from 0.879 and 0.897 to 0.897 and 0.911. The results of this study show that using the AF catalyst as a preprocessing or augmentation factor has significantly improved the performance of the basic models. This indicates the ability of AF to correct systematic or seasonal errors of the ARMA model or to add useful information to it. Furthermore, combining the AF catalyst with the GPR machine learning model has enhanced the accuracy of the GPR model, but this difference is not significant at the 95% level. This could indicate that the GPR model alone, due to its non-parametric nature and ability to learn complex nonlinear relationships, was already able to absorb a large part of the information in the data, and the added effect of AF was less noticeable in this case. However, even small improvements can be valuable in modeling complex meteorological phenomena. Overall, the GPR-AF-ARMA triple hybrid model showed the highest accuracy compared to the other models studied, followed by the ARMA-AF model, with a small difference in second place. For example, the values of R, RMSE, NS, and MAE for the 12-month SPI at Bostan station are 0.922, 0.177, 0.949, and 0.145 for the GPR-AF-ARMA model, respectively, and 0.896, 0.215, 0.909, and 0.185 for the ARMA-AF model, respectively. These results confirm the superiority of the hybrid approach that utilizes the nonlinear relationship learning capabilities of GPR, the corrective ability of AF, and the time series modeling power of ARMA. The ARMA-AF model also performed best among the triple models, indicating the significant effectiveness of combining AF with the classical ARMA model. These findings emphasize that an intelligent combination of different models can overcome the limitations of single models and achieve more accurate forecasts in the field of meteorological drought. On the other hand, the dual GPR-ARMA hybrid model yielded the lowest accuracy among the models studied. This finding provides an important insight, indicating that directly combining a complex machine learning model (GPR) with a classical time series model (ARMA) without an intermediate or correction layer, such as AF, for modeling the SPI meteorological drought index did not yield a desirable output. This may be due to inconsistencies in how the two models model the data or the inability of GPR to extract information that can be effectively combined with the ARMA model. This result highlights the importance of how and when this combination is made, and perhaps highlights the need for intermediate methods or targeted preprocessing. The results of this section are consistent with some studies, and in examining drought using integrated models based on climate data, they reported a significant superiority of integrated models over individual models (Bazrafshan et al. 2015; Hosseini-Moghari et al. 2016; Mohammadi et al. 2022; Mousazadeh et al. 2023; Gul et al. 2023).

Pre-publication Version

Table 2. Statistical results of input data to the ARMA model for predicting the SPI index

Test dataset				Train dataset				Combination number	Station
R	NS	MAE	RMSE	R	NS	MAE	RMSE		
0.543	0.612	0.376	0.403	0.593	0.641	0.342	0.381	SPI_{12}	Abadan
0.539	0.604	0.381	0.409	0.587	0.632	0.345	0.387	SPI_6	
0.533	0.593	0.388	0.414	0.581	0.624	0.353	0.392	SPI_3	
0.528	0.588	0.392	0.419	0.573	0.616	0.366	0.397	SPI_1	
0.542	0.611	0.377	0.405	0.592	0.638	0.342	0.382	SPI_{12}	Bostan
0.538	0.602	0.382	0.411	0.585	0.631	0.346	0.388	SPI_6	
0.532	0.591	0.389	0.416	0.579	0.623	0.354	0.393	SPI_3	
0.527	0.584	0.393	0.421	0.572	0.614	0.368	0.398	SPI_1	
0.541	0.609	0.378	0.406	0.592	0.636	0.344	0.383	SPI_{12}	Ahvaz
0.537	0.602	0.383	0.413	0.584	0.629	0.348	0.389	SPI_6	
0.531	0.590	0.391	0.418	0.577	0.622	0.355	0.394	SPI_3	
0.526	0.583	0.394	0.423	0.571	0.612	0.371	0.399	SPI_1	
0.539	0.608	0.379	0.407	0.591	0.633	0.345	0.385	SPI_{12}	Bandar mahshahr
0.536	0.601	0.385	0.415	0.583	0.626	0.351	0.389	SPI_6	
0.529	0.588	0.393	0.421	0.576	0.621	0.357	0.395	SPI_3	
0.525	0.581	0.397	0.425	0.569	0.609	0.374	0.401	SPI_1	
0.538	0.607	0.379	0.408	0.588	0.632	0.346	0.388	SPI_{12}	Omidiyeh
0.535	0.599	0.387	0.417	0.581	0.624	0.352	0.391	SPI_6	
0.528	0.585	0.395	0.422	0.575	0.618	0.359	0.396	SPI_3	
0.523	0.579	0.399	0.426	0.568	0.607	0.377	0.402	SPI_1	
0.537	0.605	0.381	0.409	0.586	0.632	0.347	0.391	SPI_{12}	Ramhormoz
0.534	0.596	0.388	0.418	0.579	0.623	0.353	0.393	SPI_6	
0.527	0.584	0.396	0.423	0.574	0.616	0.361	0.397	SPI_3	
0.522	0.577	0.401	0.429	0.565	0.605	0.378	0.403	SPI_1	
0.536	0.603	0.392	0.411	0.585	0.631	0.351	0.394	SPI_{12}	Masjed soleyman
0.533	0.594	0.396	0.421	0.576	0.622	0.354	0.395	SPI_6	
0.523	0.582	0.402	0.425	0.573	0.615	0.362	0.398	SPI_3	
0.518	0.575	0.408	0.433	0.563	0.604	0.379	0.406	SPI_1	
0.534	0.602	0.393	0.416	0.584	0.629	0.352	0.396	SPI_{12}	Dezful
0.531	0.593	0.397	0.422	0.575	0.621	0.355	0.398	SPI_6	
0.521	0.581	0.404	0.428	0.571	0.614	0.364	0.402	SPI_3	
0.514	0.574	0.411	0.435	0.561	0.603	0.381	0.411	SPI_1	

Pre-publication Version

Table 3. Statistical results of input data to the ARMA-GPR hybrid model for predicting the SPI index

Test dataset				Train dataset				Combination number	Station
R	NS	MAE	RMSE	R	NS	MAE	RMSE		
0.503	0.601	0.403	0.457	0.541	0.624	0.387	0.436	SPI_{12}	Abadan
0.497	0.594	0.409	0.462	0.536	0.618	0.392	0.441	SPI_6	
0.492	0.585	0.414	0.468	0.531	0.612	0.398	0.445	SPI_3	
0.484	0.574	0.421	0.474	0.524	0.604	0.404	0.449	SPI_1	
0.502	0.599	0.404	0.459	0.539	0.622	0.388	0.438	SPI_{12}	Bostan
0.496	0.593	0.411	0.463	0.534	0.617	0.393	0.442	SPI_6	
0.491	0.584	0.415	0.469	0.529	0.611	0.399	0.446	SPI_3	
0.483	0.573	0.422	0.425	0.523	0.603	0.405	0.451	SPI_1	
0.501	0.597	0.406	0.461	0.538	0.621	0.389	0.439	SPI_{12}	Ahvaz
0.495	0.592	0.413	0.464	0.533	0.616	0.394	0.443	SPI_6	
0.489	0.583	0.417	0.471	0.528	0.609	0.401	0.448	SPI_3	
0.481	0.571	0.423	0.477	0.522	0.602	0.407	0.452	SPI_1	
0.501	0.595	0.407	0.463	0.537	0.619	0.392	0.441	SPI_{12}	Bandar mahshahr
0.494	0.591	0.414	0.464	0.532	0.614	0.395	0.444	SPI_6	
0.488	0.582	0.418	0.472	0.526	0.607	0.402	0.449	SPI_3	
0.479	0.569	0.425	0.478	0.521	0.601	0.408	0.453	SPI_1	
0.501	0.594	0.408	0.464	0.536	0.617	0.394	0.442	SPI_{12}	Omidiyeh
0.493	0.589	0.415	0.465	0.531	0.613	0.397	0.445	SPI_6	
0.487	0.581	0.421	0.473	0.525	0.606	0.403	0.451	SPI_3	
0.477	0.568	0.427	0.479	0.519	0.599	0.409	0.454	SPI_1	
0.499	0.593	0.409	0.465	0.535	0.616	0.395	0.443	SPI_{12}	Ramhormoz
0.492	0.588	0.417	0.466	0.529	0.612	0.399	0.446	SPI_6	
0.486	0.579	0.424	0.474	0.524	0.605	0.406	0.452	SPI_3	
0.475	0.566	0.431	0.481	0.518	0.598	0.412	0.455	SPI_1	
0.498	0.592	0.411	0.466	0.534	0.615	0.397	0.444	SPI_{12}	Masjed soleyman
0.491	0.586	0.418	0.467	0.528	0.611	0.401	0.448	SPI_6	
0.485	0.577	0.425	0.475	0.516	0.604	0.407	0.453	SPI_3	
0.474	0.564	0.432	0.482	0.515	0.596	0.416	0.456	SPI_1	
0.497	0.591	0.412	0.467	0.532	0.613	0.398	0.447	SPI_{12}	Dezful
0.489	0.585	0.421	0.468	0.527	0.609	0.402	0.449	SPI_6	
0.484	0.574	0.426	0.476	0.514	0.603	0.409	0.454	SPI_3	
0.473	0.561	0.433	0.483	0.512	0.594	0.417	0.463	SPI_1	

Pre-publication Version

Table 4. Statistical results of input data to the GPR model for predicting the SPI index

Test dataset				Train dataset				Combination number	Station
R	NS	MAE	RMSE	R	NS	MAE	RMSE		
0.817	0.843	0.242	0.274	0.833	0.861	0.221	0.256	SPI_{12}	Abadan
0.815	0.841	0.243	0.275	0.832	0.859	0.224	0.259	SPI_6	
0.814	0.839	0.244	0.277	0.831	0.857	0.227	0.262	SPI_3	
0.813	0.838	0.245	0.281	0.829	0.853	0.231	0.263	SPI_1	
0.816	0.842	0.247	0.276	0.831	0.858	0.222	0.257	SPI_{12}	Bostan
0.814	0.841	0.249	0.277	0.828	0.856	0.225	0.259	SPI_6	
0.812	0.837	0.251	0.281	0.827	0.854	0.228	0.264	SPI_3	
0.811	0.836	0.254	0.283	0.826	0.849	0.232	0.265	SPI_1	
0.815	0.841	0.248	0.277	0.831	0.855	0.223	0.258	SPI_{12}	Ahvaz
0.813	0.839	0.251	0.279	0.827	0.855	0.226	0.261	SPI_6	
0.811	0.835	0.253	0.282	0.826	0.846	0.229	0.266	SPI_3	
0.809	0.834	0.257	0.285	0.825	0.843	0.234	0.267	SPI_1	
0.814	0.841	0.249	0.278	0.829	0.851	0.224	0.259	SPI_{12}	Bandar mahshahr
0.812	0.837	0.252	0.281	0.824	0.849	0.227	0.263	SPI_6	
0.808	0.833	0.255	0.283	0.823	0.845	0.231	0.269	SPI_3	
0.807	0.832	0.258	0.288	0.821	0.841	0.235	0.271	SPI_1	
0.813	0.841	0.251	0.279	0.828	0.848	0.225	0.262	SPI_{12}	Omidiyeh
0.811	0.836	0.253	0.282	0.822	0.847	0.228	0.265	SPI_6	
0.806	0.832	0.257	0.285	0.819	0.843	0.232	0.272	SPI_3	
0.805	0.831	0.261	0.291	0.817	0.839	0.236	0.273	SPI_1	
0.812	0.839	0.252	0.281	0.827	0.846	0.227	0.263	SPI_{12}	Ramhormoz
0.809	0.835	0.255	0.284	0.821	0.844	0.229	0.266	SPI_6	
0.805	0.831	0.259	0.287	0.818	0.842	0.233	0.273	SPI_3	
0.804	0.829	0.262	0.293	0.816	0.838	0.237	0.275	SPI_1	
0.811	0.838	0.253	0.282	0.826	0.845	0.228	0.264	SPI_{12}	Masjed soleyman
0.808	0.834	0.257	0.285	0.819	0.843	0.235	0.267	SPI_6	
0.804	0.828	0.261	0.289	0.817	0.841	0.238	0.275	SPI_3	
0.803	0.827	0.264	0.299	0.815	0.837	0.241	0.278	SPI_1	
0.809	0.837	0.255	0.283	0.824	0.844	0.229	0.265	SPI_{12}	Dezful
0.807	0.833	0.258	0.286	0.818	0.842	0.236	0.268	SPI_6	
0.803	0.826	0.262	0.293	0.816	0.839	0.242	0.276	SPI_3	
0.802	0.823	0.265	0.299	0.814	0.835	0.246	0.279	SPI_1	

Pre-publication Version

Table 5. Statistical results of input data to the GPR-AF hybrid model for predicting the SPI index

Test dataset				Train dataset				Combination number	Station
R	NS	MAE	RMSE	R	NS	MAE	RMSE		
0.843	0.873	0.218	0.249	0.866	0.897	0.188	0.234	SPI_{12}	Abadan
0.842	0.872	0.223	0.253	0.864	0.894	0.193	0.239	SPI_6	
0.842	0.868	0.228	0.259	0.863	0.886	0.197	0.244	SPI_3	
0.841	0.863	0.233	0.263	0.861	0.883	0.203	0.257	SPI_1	
0.842	0.872	0.219	0.251	0.865	0.896	0.189	0.235	SPI_{12}	Bostan
0.841	0.871	0.224	0.254	0.863	0.892	0.194	0.241	SPI_6	
0.839	0.865	0.229	0.261	0.862	0.885	0.198	0.245	SPI_3	
0.837	0.862	0.235	0.265	0.859	0.881	0.205	0.258	SPI_1	
0.841	0.871	0.221	0.252	0.864	0.895	0.191	0.237	SPI_{12}	Ahvaz
0.837	0.869	0.225	0.255	0.861	0.891	0.195	0.242	SPI_6	
0.835	0.864	0.231	0.262	0.858	0.884	0.201	0.246	SPI_3	
0.833	0.861	0.237	0.266	0.853	0.879	0.207	0.259	SPI_1	
0.839	0.871	0.223	0.254	0.863	0.893	0.192	0.239	SPI_{12}	Bandar mahshahr
0.836	0.868	0.227	0.257	0.859	0.889	0.196	0.243	SPI_6	
0.833	0.863	0.234	0.263	0.856	0.882	0.202	0.247	SPI_3	
0.831	0.859	0.241	0.267	0.851	0.876	0.208	0.261	SPI_1	
0.838	0.869	0.225	0.256	0.862	0.892	0.194	0.241	SPI_{12}	Omidiyeh
0.832	0.866	0.228	0.259	0.858	0.888	0.198	0.244	SPI_6	
0.828	0.861	0.235	0.265	0.855	0.881	0.203	0.248	SPI_3	
0.824	0.858	0.242	0.271	0.848	0.874	0.209	0.263	SPI_1	
0.836	0.866	0.227	0.257	0.861	0.891	0.195	0.242	SPI_{12}	Ramhormoz
0.831	0.864	0.229	0.261	0.857	0.886	0.199	0.245	SPI_6	
0.826	0.859	0.236	0.266	0.853	0.879	0.204	0.249	SPI_3	
0.823	0.856	0.244	0.273	0.844	0.873	0.211	0.265	SPI_1	
0.833	0.865	0.228	0.259	0.859	0.889	0.195	0.243	SPI_{12}	Masjed soleyman
0.829	0.862	0.231	0.262	0.855	0.884	0.201	0.247	SPI_6	
0.825	0.858	0.237	0.269	0.852	0.877	0.206	0.251	SPI_3	
0.821	0.855	0.245	0.275	0.843	0.872	0.213	0.266	SPI_1	
0.832	0.864	0.229	0.261	0.855	0.885	0.198	0.244	SPI_{12}	Dezful
0.828	0.861	0.232	0.264	0.851	0.883	0.202	0.248	SPI_6	
0.824	0.857	0.238	0.271	0.842	0.874	0.207	0.252	SPI_3	
0.818	0.853	0.246	0.277	0.839	0.871	0.214	0.267	SPI_1	

Pre-publication Version

Table 6. Statistical results of input data to the ARMA-AF hybrid model for predicting the SPI index

Test dataset				Train dataset				Combination number	Station
R	NS	MAE	RMSE	R	NS	MAE	RMSE		
0.897	0.911	0.184	0.213	0.921	0.937	0.157	0.197	SPI_{12}	Abadan
0.893	0.907	0.187	0.219	0.917	0.933	0.161	0.202	SPI_6	
0.884	0.902	0.191	0.222	0.913	0.928	0.164	0.204	SPI_3	
0.879	0.897	0.196	0.227	0.909	0.925	0.169	0.209	SPI_1	
0.896	0.909	0.185	0.215	0.919	0.936	0.158	0.198	SPI_{12}	Bostan
0.892	0.905	0.188	0.221	0.916	0.932	0.162	0.203	SPI_6	
0.883	0.901	0.192	0.224	0.912	0.927	0.165	0.207	SPI_3	
0.877	0.896	0.197	0.228	0.907	0.924	0.171	0.212	SPI_1	
0.894	0.908	0.187	0.216	0.917	0.935	0.159	0.199	SPI_{12}	Ahvaz
0.891	0.903	0.189	0.222	0.916	0.931	0.164	0.205	SPI_6	
0.882	0.899	0.193	0.225	0.909	0.926	0.166	0.209	SPI_3	
0.875	0.894	0.199	0.229	0.904	0.922	0.173	0.214	SPI_1	
0.893	0.907	0.188	0.217	0.916	0.934	0.161	0.201	SPI_{12}	Bandar mahshahr
0.889	0.902	0.191	0.223	0.914	0.929	0.165	0.207	SPI_6	
0.881	0.896	0.195	0.226	0.908	0.925	0.168	0.211	SPI_3	
0.874	0.893	0.201	0.231	0.903	0.921	0.174	0.217	SPI_1	
0.892	0.906	0.189	0.218	0.915	0.933	0.162	0.203	SPI_{12}	Omidiyeh
0.888	0.901	0.193	0.224	0.913	0.928	0.166	0.211	SPI_6	
0.879	0.894	0.197	0.227	0.907	0.924	0.171	0.214	SPI_3	
0.873	0.891	0.202	0.234	0.902	0.919	0.177	0.218	SPI_1	
0.891	0.905	0.191	0.219	0.912	0.931	0.163	0.204	SPI_{12}	Ramhormoz
0.887	0.899	0.195	0.225	0.911	0.927	0.168	0.213	SPI_6	
0.878	0.893	0.198	0.229	0.906	0.923	0.172	0.217	SPI_3	
0.873	0.889	0.203	0.235	0.901	0.917	0.179	0.221	SPI_1	
0.889	0.904	0.192	0.221	0.912	0.929	0.164	0.205	SPI_{12}	Masjed soleyman
0.885	0.897	0.196	0.227	0.909	0.925	0.169	0.214	SPI_6	
0.876	0.892	0.199	0.231	0.905	0.921	0.173	0.218	SPI_3	
0.872	0.887	0.204	0.237	0.899	0.915	0.181	0.222	SPI_1	
0.887	0.903	0.193	0.222	0.911	0.928	0.165	0.207	SPI_{12}	Dezful
0.884	0.896	0.198	0.228	0.908	0.924	0.171	0.215	SPI_6	
0.875	0.891	0.201	0.232	0.903	0.919	0.174	0.219	SPI_3	
0.871	0.886	0.205	0.239	0.895	0.913	0.183	0.223	SPI_1	

Pre-publication Version

Table 7. Statistical results of input data to the combined GPR-AF-ARMA model for predicting the SPI index

Test dataset				Train dataset				Combination number	Station
R	NS	MAE	RMSE	R	NS	MAE	RMSE		
0.923	0.951	0.144	0.176	0.966	0.984	0.125	0.155	SPI_{12}	Abadan
0.917	0.948	0.148	0.181	0.961	0.979	0.128	0.163	SPI_6	
0.913	0.943	0.152	0.185	0.955	0.973	0.132	0.169	SPI_3	
0.909	0.939	0.155	0.189	0.942	0.969	0.137	0.174	SPI_1	
0.922	0.949	0.145	0.177	0.965	0.983	0.127	0.156	SPI_{12}	Bostan
0.916	0.947	0.149	0.182	0.959	0.977	0.131	0.165	SPI_6	
0.912	0.942	0.153	0.186	0.954	0.972	0.134	0.171	SPI_3	
0.908	0.937	0.156	0.191	0.941	0.968	0.139	0.178	SPI_1	
0.921	0.948	0.146	0.178	0.963	0.982	0.128	0.158	SPI_{12}	Ahvaz
0.915	0.946	0.151	0.183	0.958	0.976	0.132	0.166	SPI_6	
0.911	0.941	0.154	0.187	0.953	0.971	0.135	0.173	SPI_3	
0.907	0.936	0.158	0.192	0.941	0.966	0.141	0.179	SPI_1	
0.919	0.947	0.147	0.179	0.962	0.981	0.129	0.159	SPI_{12}	Bandar mahshahr
0.914	0.945	0.152	0.184	0.957	0.975	0.133	0.167	SPI_6	
0.909	0.939	0.156	0.188	0.952	0.969	0.136	0.174	SPI_3	
0.906	0.935	0.159	0.193	0.939	0.965	0.142	0.181	SPI_1	
0.918	0.946	0.149	0.181	0.961	0.979	0.131	0.161	SPI_{12}	Omidiyeh
0.913	0.944	0.153	0.185	0.956	0.974	0.134	0.169	SPI_6	
0.908	0.938	0.157	0.189	0.951	0.968	0.138	0.175	SPI_3	
0.904	0.934	0.161	0.194	0.937	0.964	0.144	0.182	SPI_1	
0.916	0.945	0.151	0.182	0.959	0.977	0.132	0.163	SPI_{12}	Ramhormoz
0.912	0.943	0.154	0.186	0.953	0.973	0.136	0.171	SPI_6	
0.907	0.937	0.158	0.191	0.949	0.967	0.139	0.177	SPI_3	
0.903	0.933	0.162	0.195	0.935	0.962	0.145	0.183	SPI_1	
0.915	0.944	0.151	0.184	0.958	0.976	0.133	0.165	SPI_{12}	Masjed soleyman
0.911	0.942	0.154	0.187	0.952	0.972	0.137	0.172	SPI_6	
0.906	0.936	0.159	0.192	0.947	0.966	0.141	0.179	SPI_3	
0.902	0.932	0.165	0.197	0.934	0.961	0.146	0.185	SPI_1	
0.914	0.941	0.151	0.185	0.957	0.975	0.134	0.167	SPI_{12}	Dezful
0.909	0.935	0.155	0.188	0.951	0.971	0.139	0.173	SPI_6	
0.905	0.929	0.161	0.193	0.946	0.965	0.143	0.182	SPI_3	
0.901	0.927	0.166	0.198	0.932	0.959	0.147	0.187	SPI_1	

Pre-publication Version

The SPI prediction results demonstrated the superior performance of the GPR-AF-ARMA hybrid model across the eight studied stations in Khuzestan Province. The model achieved the highest R and NSE values and the lowest RMSE and MAE values among all investigated models, indicating

its strong capability in meteorological drought forecasting. The superior performance of the proposed hybrid framework can be attributed to the complementary strengths of its constituent components. The GPR component effectively captures complex nonlinear relationships and uncertainty structures within SPI time series, while the ARMA component models the linear temporal dependencies and stochastic characteristics of drought sequences. In addition, the AF optimization algorithm improves parameter adjustment and enhances the overall learning process of the hybrid framework. Consequently, the integration of these approaches enables the model to simultaneously represent nonlinear, stochastic, and temporal patterns in meteorological drought data more effectively than standalone models.

Among the investigated models, the ARMA-AF hybrid model showed the second-best performance, with results very close to those of the GPR-AF-ARMA model. This finding indicates that incorporating the AF optimization mechanism significantly improves the predictive capability of the conventional ARMA model by reducing modeling errors and improving parameter calibration. However, the relatively small difference between the ARMA-AF and GPR-AF-ARMA models suggests that the increase in computational complexity, training time, and implementation cost associated with the triple hybrid structure may not always be operationally justified in practical applications. Therefore, the ARMA-AF model may represent a cost-effective and computationally efficient alternative for operational drought forecasting in Khuzestan Province.

These findings emphasize that model evaluation should not rely solely on predictive accuracy but should also consider computational efficiency, implementation feasibility, and operational applicability. In many real-world forecasting systems, simpler models with slightly lower accuracy may be preferred because of their lower computational demand and easier implementation. According to AghaKouchak et al. (2022), developing robust bottom-up forecasting approaches and accounting for uncertainty in drought prediction are more important than merely reproducing historical events. Similarly, incorporating climatic randomness and uncertainty into predictive frameworks has been shown to improve forecasting reliability. Nevertheless, further studies are still required to better understand the spatial and temporal complexities associated with drought prediction under climate change conditions (Mishra & Singh, 2011).

The results also revealed that longer SPI time scales, particularly SPI-12, produced more reliable forecasting results than short-term indices. In arid and semi-arid environments such as Khuzestan Province, precipitation is highly seasonal and exhibits substantial spatial and temporal variability. Therefore, longer accumulation periods are more capable of representing persistent precipitation deficits and long-term drought behavior. In contrast, short-term SPI series are strongly influenced by seasonal precipitation fluctuations and may not accurately reflect sustained drought conditions. Fig. 4 presents the observed and predicted SPI-12 values for the testing datasets at the studied stations. The relationship between observed and predicted values was evaluated using the 45-degree bisector line. The ARMA-GPR model exhibited the greatest dispersion from the bisector line, indicating lower predictive accuracy and weaker agreement between observed and simulated values. In contrast, the GPR-AF-ARMA model showed the highest concentration of points around the bisector line, reflecting its superior predictive stability, lower uncertainty, and stronger agreement with the observed SPI values. These results further confirm the effectiveness of the proposed hybrid framework in capturing the complex hydroclimatic behavior of meteorological drought in Khuzestan Province.

Pre-publication Version

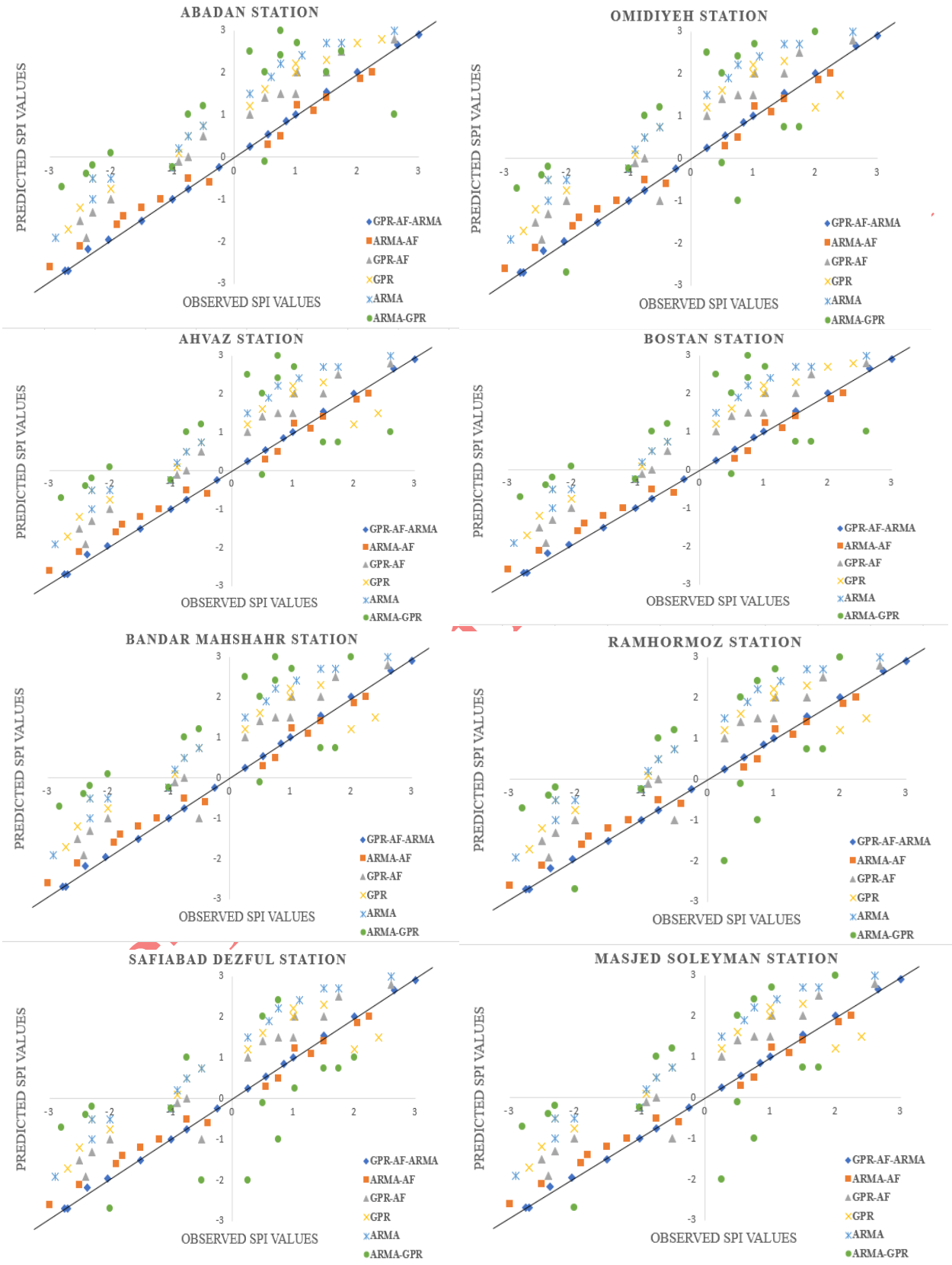


Fig 4. Comparison of observed and predicted SPI values using the studied models

Conclusion

In the present study, the triple hybrid GPR-AF-ARMA model was evaluated for meteorological drought forecasting at eight synoptic stations in Khuzestan Province during the 1989–2020 period. The obtained results demonstrated that the GPR-AF-ARMA model achieved the highest predictive accuracy among the investigated models, followed closely by the ARMA-AF hybrid model. These findings confirm the effectiveness of hybrid forecasting approaches that integrate the nonlinear learning capability of GPR, the optimization performance of the AF algorithm, and the temporal modeling strength of ARMA.

Although the GPR-AF-ARMA model produced the best overall performance, the ARMA-AF model generated highly comparable results with lower computational complexity, shorter training time, and reduced implementation cost. Therefore, the ARMA-AF framework may represent a practical and cost-effective alternative for operational meteorological drought forecasting in Khuzestan Province. This finding highlights the importance of evaluating forecasting models not only from an accuracy perspective, but also in terms of computational efficiency and operational applicability.

The results further indicate that hybrid intelligent models have substantial potential for improving drought prediction accuracy and supporting climate risk management strategies in arid and semi-arid regions. Consequently, the implementation of advanced hybrid forecasting frameworks in drought monitoring systems and early warning platforms can contribute significantly to reducing the environmental and socioeconomic impacts of drought events.

Despite the promising results obtained in this study, several opportunities remain for future research. Future investigations are recommended to evaluate the performance of advanced deep learning architectures, including Transformer-based models and recurrent neural networks, for long-term drought forecasting under complex climatic conditions. In addition, incorporating longer historical datasets and integrating additional hydroclimatic variables, such as temperature, evapotranspiration, soil moisture, and large-scale climate indices, may further improve model robustness and predictive reliability. Evaluating the proposed models under different climate change and water management scenarios could also provide valuable insights into drought resilience and adaptation planning. Furthermore, uncertainty analysis and probabilistic forecasting approaches are suggested for future studies to better quantify prediction uncertainty and improve decision-making processes in operational drought management systems.

Pre-publication Version

Declaration of competing interests

The authors declare that they have no known competing financial interests or personal relationships that could have appeared to influence the work reported in this paper.

Data availability

The data that has been used is confidential.

Funding

No funding was received for conducting this study.

References

Adnan, R. M., Dai, H. L., Kuriqi, A., Kisi, O., & Kermani, M. Z. (2023). Improving drought modeling based on new heuristic machine learning methods. *Ain Shams Engineering Journal*, 14, 1–13.

AghaKouchak, A., Pan, B., Mazdiyasni, O., Sadegh, M., Jiwa, S., Zhang, W., Love, C. A., Madadgar, S., Papalexiou, S. M., & Davis, S. J. (2022). Status and prospects for drought forecasting: Opportunities in artificial intelligence and hybrid physical–statistical forecasting. *Philosophical Transactions of the Royal Society A*, 380, 20210288. https://doi.org/10.1098/rsta.2021.0288

Babaali, H., Nohani, E., & Dehghani, R. (2024). Evaluation of the Standardized Precipitation Index with a hybrid model based on machine learning (case study: Lorestan province). *Journal of Climate Research*. https://clima.irimo.ir/article_210510_en.html?lang=fa

Bazrafshan, O., Salajegheh, A., Mahdavi, M., & Fatehi, A. (2015). A study of the efficiency of hybrid artificial neural network–stochastic models in hydrological drought forecasting using kappa statistics (case study: Gamasiab watershed basin). *Iranian Journal of Watershed Management Science*, 8(27), 35–48.

Belayneh, A., Adamowski, J., Khalil, B., & Quilty, J. (2016). Coupling machine learning methods with wavelet transforms, bootstrap, and boosting ensemble approaches for drought prediction. *Atmospheric Research*, 172, 37–47. https://doi.org/10.1016/j.atmosres.2015.12.017

Bond, N. R., Lake, P. S., & Arthington, A. H. (2008). The impacts of drought on freshwater ecosystems: An Australian perspective. *Hydrobiologia*, 600, 3–16. https://doi.org/10.1007/s10750-008-9326-z

Chang, S., Chen, H., Wu, B., Nasanbat, E., Yan, N., & Davdai, B. (2021). A practical satellite-derived vegetation drought index for arid and semi-arid grassland drought monitoring. *Remote Sensing*, 13, 414. https://doi.org/10.3390/rs13030414

Das, P., Naganna, S. R., Deka, P. C., & Pushparaj, J. (2020). Hybrid wavelet packet machine learning approaches for drought modeling. *Environmental Earth Sciences*, 79, 221. https://doi.org/10.1007/s12665-020-08971-y

Dehghani, R., Torabi-Poudeh, H., Younesi, H., & Shahinejad, B. (2020). Application of a hybrid support vector machine–artificial flora algorithm in estimating daily river flow (case study: Dez basin). *Iran Water Resources Research*, 16(2), 132–149.

Gul, E., Staiou, E., Safari, M. J. S., & Vaheddoost, B. (2023). Enhancing meteorological drought modeling accuracy using hybrid boost regression models: A case study from the Aegean region, Türkiye. *Sustainability*, 15, 11568. https://doi.org/10.3390/su151511568

Hisdal, H., Stahl, K., Tallaksen, L. M., & Demuth, S. (2001). Have streamflow droughts in Europe become more severe or frequent? *International Journal of Climatology*, 21, 317–333. https://doi.org/10.1002/joc.619

Hosseini-Moghari, S. M., & Araghinejad, S. (2016). Application of statistical, fuzzy, and perceptron neural networks in drought forecasting (case study: Gonbad-e Kavous station). *Water and Soil*, 30(1), 247–259. https://doi.org/10.22067/jsw.v30i1.37304

Liu, Q., Zhang, G., Ali, S., Wang, X., Wang, G., Pan, Z., & Zhang, J. (2019). SPI-based drought simulation and prediction using the ARMA-GARCH model. *Applied Mathematics and Computation*, 355, 96–107. https://doi.org/10.1016/j.amc.2019.02.058

McKee, T. B., Doesken, N. J., & Kleist, J. (1993). The relationship of drought frequency and duration to time scales. In *Proceedings of the 8th Conference on Applied Climatology* (pp. 179–184). Anaheim, CA, USA: American Meteorological Society.

Mishra, A. K., & Singh, V. P. (2011). Drought modeling—A review. *Journal of Hydrology*, 403, 157–175. https://doi.org/10.1016/j.jhydrol.2011.03.049

Mohammadi, J., Vafaeinezhad, A., Behzadi, S., Aghamohammadi, H., & Hemmasi, A. (2022). Drought prediction and modeling by a hybrid wavelet method and neural network algorithms. *Remote Sensing and GIS for Natural Resources*, 4(13), 87–111.

Pre-publication Version

Mousazadeh, N., Akhundali, A. M., & Ahmadi, F. (2023). Development of integrated machine learning models based on complete ensemble empirical mode decomposition method for estimating dam inflow (case study: Dez Dam). *Iranian Journal of Irrigation and Drainage, 17*(4), 685–701.

Moisa, M. B., Merga, B. B., & Gemeda, D. O. (2022). Multiple indices-based assessment of agricultural drought: A case study in Gilgel Gibe sub-basin, Southern Ethiopia. *Theoretical and Applied Climatology*, 148, 455–464. https://doi.org/10.1007/s00704-022-03962-4

Negahban, S., Mokarram, M., & Moradizadeh Kermani, R. (2024). Assessing the effects of drought hazards on rural communities surrounding Maharlu Lake, Iran. *Environmental Hazards Management*, 11(1), 1–13. https://doi.org/10.22059/jhsci.2024.374378.823

Shamloo, N., Sattari, M. T., Valizadeh Khalil, K., & Apaydin, H. (2023). Evaluation of the combined agricultural drought index (CDI), prediction methods based on satellite images via deep learning and machine learning approaches. *Water and Soil*, 37(5), 787–807. https://doi.org/10.22067/jsw.2023.82798.1293

Sun, P., Ma, Z., Zhang, Q., Singh, V. P., & Xu, C. Y. (2022). Modified drought severity index: Model improvement and its application in drought monitoring in China. *Journal of Hydrology*, 612, 128097. https://doi.org/10.1016/j.jhydrol.2022.128097

Wilhite, D. A., Svoboda, M. D., & Hayes, M. J. (2007). Understanding the complex impacts of drought: A key to enhancing drought mitigation and preparedness. *Water Resources Management, 21*, 763–774. https://doi.org/10.1007/s11269-006-9076-5

Zhu, S., Luo, X., Xu, Z., & Ye, L. (2019). Seasonal streamflow forecasts using mixture-kernel GPR and advanced methods of input variable selection. *Hydrology Research*, 50(1), 200–214. https://doi.org/10.2166/nh.2018.023

Pre-publication Version